Characterizing the Survey Strategy and Initial Orbit Determination Abilities of the NASA MCAT Telescope for Geosynchronous Orbital Debris Environmental Studies

James Frith
University of Texas El Paso
Jacobs JETS Contract, NASA Johnson Space Center
2224 Bay Area Blvd, Houston, TX 77058
Ed Barker
LZ Technology, Inc. 1110 NASA Pkwy Ste. 650, Houston, Texas 77058
Heather Cowardin
University of Texas El Paso
Jacobs JETS Contract, NASA Johnson Space Center
2224 Bay Area Blvd, Houston, TX 77058
Brent Buckalew
Jacobs, NASA Johnson Space Center, 2224 Bay Area Blvd, Houston, TX 77058
Phillip Anz-Meador
Jacobs, NASA Johnson Space Center, 2224 Bay Area Blvd, Houston, TX 77058
Susan Lederer
NASA Johnson Space Center, 2101 NASA Parkway, Houston TX 77058

ABSTRACT

The National Aeronautics and Space Administration (NASA) Orbital Debris Program Office (ODPO) recently commissioned the Meter Class Autonomous Telescope (MCAT) on Ascension Island with the primary goal of obtaining population statistics of the geosynchronous (GEO) orbital debris environment. To help facilitate this, studies have been conducted using MCAT's known and projected capabilities to estimate the accuracy and timeliness in which it can survey the GEO environment, including collected weather data and the proposed observational data collection cadence. To optimize observing cadences and probability of detection, on-going work using a simulated GEO debris population sampled at various cadences are run through the Constrained Admissible Region Multi Hypotheses Filter (CAR-MHF). The orbits computed from the results are then compared to the simulated data to assess MCAT's ability to determine accurately the orbits of debris at various sample rates. The goal of this work is to discriminate GEO and near-GEO objects from GEO transfer orbit objects that can appear as GEO objects in the environmental models due to the short arc observation and an assumed circular orbit. The specific methods and results are presented here.

1. INTRODUCTION

1.1 Previous Work

To aid in the characterization of the geosynchronous orbital debris environment, NASA employed the use of the Michigan Orbital DEbris Survey Telescope (MODEST), the University of Michigan's 0.61-m aperture Curtis-Schmidt telescope at the Cerro Tololo Inter-American Observatory in Chile. The use of MODEST started in February 2001 and continued thru 2014. MODEST used a 2048 by 2048-pixel charged coupled device camera with a 1.3° by 1.3° field of view (FOV) from 2001-2010. After a camera and detector upgrade, all survey data collected in 2013-2014 were acquired with a thinned, backside illuminated Charge-Coupled Device (CCD) with 1.45 arc-seconds/pixel and a FOV of 1.6° by 1.6°. This system is capable of detecting objects fainter than 18th magnitude (R filter) using a 5-s integration. This corresponds to a 20-cm diameter, 0.175-albedo object at 36,000 km altitude assuming a diffuse Lambertian phase function.

1.2 MODEST Observing Strategy

Previous studies [1, 2] provide compelling arguments that most uncontrolled debris objects in geosynchronous orbits (GEO) should have inclinations (INCs) less than or equal to 15 degrees. Orbits of uncontrolled GEO objects oscillate around the stable Laplacian plane, which has an INC of 7.5 degrees with respect to the equatorial plane. This oscillation is dominated by the combined effects of the Earth's oblateness (J2 term) and solar and lunar perturbations. The INC oscillation period is about 50 years. During the first 25 years, an uncontrolled object with an initial INC of 0 degrees will gradually increase in INC until its INC has peaked at 15 degrees. During the next 25 years, this same object's INC will gradually decrease until it has returned to its original INC, in this case 0 degrees, and it will begin its oscillation cycle again. Most uncontrolled objects with different initial INC values will follow the same 50-year pattern of increasing their INC to 15 degrees, decreasing to 0 degrees, and then returning to their original INC. (There are some cases in which the INC will initially decrease to 0 degrees.) Depending on the insertion Right Ascension of the Ascending Node (RAAN), an uncontrolled object's oscillation can be out of phase with other objects, although these examples are few.

From MODEST's location, orbital longitudes from 25° W. to 135° W. are accessible. Each night, MODEST was pointed toward a specific Right Ascension (RA) and Declination (DEC) that was the closest to the anti-solar point as possible without observing a location in the Earth's shadow (depending on the time of year, this approximated to about 18 degrees from the center of the anti-solar point)[3, 4]. The telescope then tracked sidereally at that location for the night. However, on nights near the equinoxes when the shadow overlapped the region of interest near the anti-solar point, two RA fields were observed by switching locations halfway through the night, with the first half of the night leading the shadow of the Earth and the second half of the night trailing the shadow. Typically the separation from the anti-solar point was 1 hour in RA. All telescope-pointing locations were determined prior to the start of the run. The location of the Moon also played a role as to when observations can occur. As a general rule, observations took place ±1 week around the new moon.

Fig. 1 shows a snapshot view as seen from MODEST of the cataloged GEO objects on a given night in 2007. The colored squares indicate the telescope pointings in RA and DEC for each observing night while Fig. 1 gives a general view of the coverage of the GEO belt.

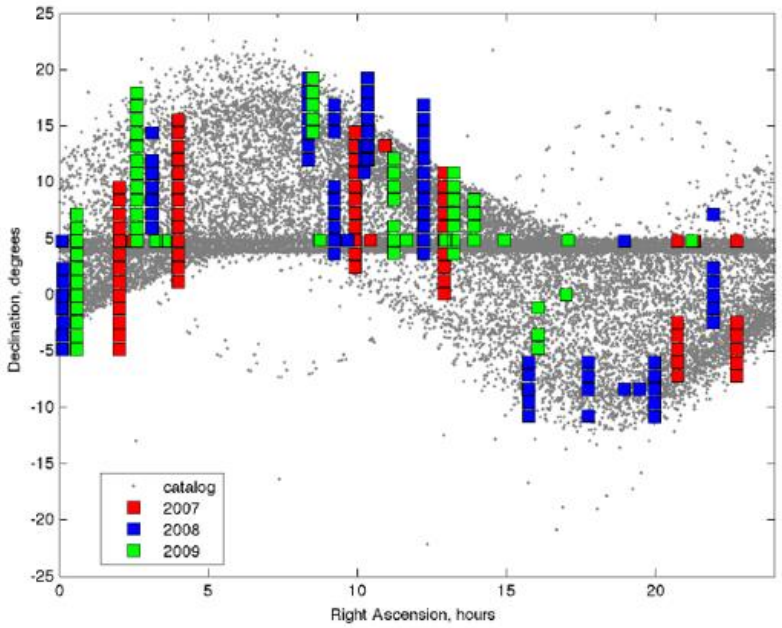

Fig. 1. Location of observed field centers using MODEST during the 2007-2009 campaign period.

1.3 Definition of the Expectation Value Coverage

To quantitatively determine the observational coverage of the INC/RAAN space, the National Aeronautics and Space Administration (NASA) Orbital Debris Program Office ODPO developed code that predicts the Expectation Value (EV) of coverage (This has been referred to as "probability of coverage" in a previous publication [5]). The EV is defined as the fraction of time during an orbit that the telescope system observed an artificial target with a given INC and RAAN. The computer code predicts what INC/RAAN-space a telescope can observe given the telescope site and system, observational date, universal time (UT), RA, and geocentric latitude. A field center (FC) is generated for each INC/RAAN pointing. An angular state vector (SV[FC]) to the field center from the telescope is calculated based on the given parameters. To sample the INC/RAAN space, a series of artificial GEO orbits (mean motion = 1.0027, a=42,164.2 km, eccentricity = 0) are calculated by varying the INC values from 0 to 30 degrees in steps of 1 degree for each value of RAAN between 0 and 360 degrees in steps of 0.25 degree. Target State Vectors (TSVs[INC/RANN]) are then calculated for each telescope pointing and INC/RAAN pair.

The code compares the fields defined by the field center positions by using the FOV of the camera system with the positions of the targets generated along the artificial orbits. The FOV is defined as the super-scribed circle for square CCD arrays or the super-scribed ellipse for rectangular CCDs using the average of the x, y dimensions. The criteria for detection of an artificial target is defined as four consecutive camera frames where the angular distances between SV(FC) and TSV(INC/RAAN) are smaller in both X (angular distance, phi) and Y (angular distance theta) as defined by the FOV. If both angles are less than their corresponding CCD dimension, the target is considered detected. If the target is found within four consecutive fields and within the rate box (± 5 arcsec in RA and ± 2 arcsec in DEC), then a detection is recorded.

The program calculates the EV that the telescope system observed for a particular INC/RAAN as defined by the artificial target. The EV of detection is quantitatively defined as the sum of detections divided by 1000 within a given FC. The EV is scaled to 1000, thus assuming there were 1000 possible detections along the ~ 24-hour orbit defined by a mean motion of 1.0027. This scaling number could be increased with a very significant increase in computational time.

Fig. 2 shows an example of the EV to define the observational coverage. If the EV is equal to 1.0, then the observational coverage is complete or all artificial orbits defined by an INC/RAAN pair have been detected. If EV is greater than 1.0 then the observational coverage is over sampled. The EV value is color-coded in and scaled to 1.0. The actual detections are noted by black dots for objects correlated with the SSN catalogue (CTs) and open circles for targets that could not be correlated with a catalogued object (UCTs). These detections demonstrate the oscillation in INC/RAAN space by UCTs as proposed by [1].

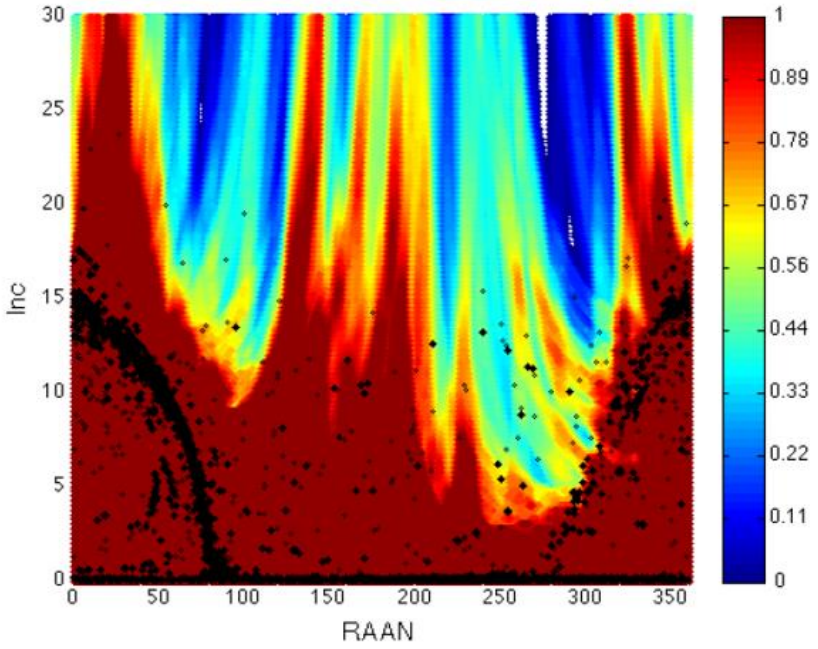

Fig.2. Expectation Value of finding specific orbits (INC/RAAN pairs) based on FC location during the 2007-2009 MODEST observing.

Due to the short orbital arc over which observations are made, the eccentricity of the object's orbit is extremely difficult to measure accurately. Therefore, a circular orbit was assumed when calculating the orbital elements.

In this paper, we apply the capabilities of the Eugene Stansbery (ES) Meter Class Autonomous Telescope (MCAT) and the EV process developed for MODEST to produce the same output for NASA models but with MCAT results. These EVs will be used to generate theoretical predictions for the complete coverage of INC vs. RAAN space as defined by the MODEST observations. We incorporate the past year's weather statistics into the time necessary for complete coverage. Finally, we discuss our future and ongoing work to better statistically sample the populations of orbital debris with more eccentric orbits..

2. MCAT Overview

2.1 MCAT

The MCAT telescope is a 1.3m f/4 telescope, sensitive from 0.3 to 1.06 μm. Equipped with a 4 k by 4 k Spectral Instrument imaging camera, it has a 41 by 41arcmin FOV, Sloan Digital Sky Survey (SDSS) g′r′i′z′ filters, and Johnson/Kron-Cousins BVRI filters. MCAT is capable of fast tracking for observing at any orbital regime. Located on Ascension Island in the middle of the Atlantic Ocean at nearly 8° S. latitude, it is also well suited for orbital inclinations down to and including Low Inclination low Earth orbit (LEO) (*i.e.*, LILO). MCAT is capable of using Time Delay Integration techniques [6] in its search for debris as well as tracking at a user-defined non-sidereal rate.

With installation completed mid-2015, MCAT is in its engineering phase of operations, undergoing extensive algorithm testing and verification of all systems.

3. Simulated MCAT GEO Survey and Calculated Expectation Value

The goal of this exercise is to determine what amount of observational coverage is required to reach EV $\geq$ 1.0 across the GEO region of interest using the observational characteristics of MCAT. To achieve this, a series of preliminary prediction simulations have been run for MCAT's site and instrumentation to determine what observational coverage is needed to reach a value of EV $\geq$ 1 for regions of interest in the INC vs. RAAN space. These simulations have been run using the same process and procedures that were used for MODEST observing runs, as discussed in Section 1.

The following assumptions were used for the simulations:

- Observational campaigns consisted of 23 nights per month centered on the new moon;
- Two RA regions were observed each night: 1 hour east of the anti-solar point and 1 hour west of the anti-solar point;
- Each RA region was observed for 4 hours per night; and
- GEO DECs were chosen each night to cover the band of active GEO targets.

Fig. 3. illustrates the cataloged GEO targets as dots and the MCAT FOV (0.68°) as red squares. In general, it took 23 FOVs or 23 GEO declinations to cover the GEO band. Thus, the choice of 23 observing nights per new moon period was accurate. In some cases near the maxima/minima of the GEO band up to 26 FOVs were required and additional nights were added to the simulation for that new moon period. It was assumed that the FOVs did not overlap.

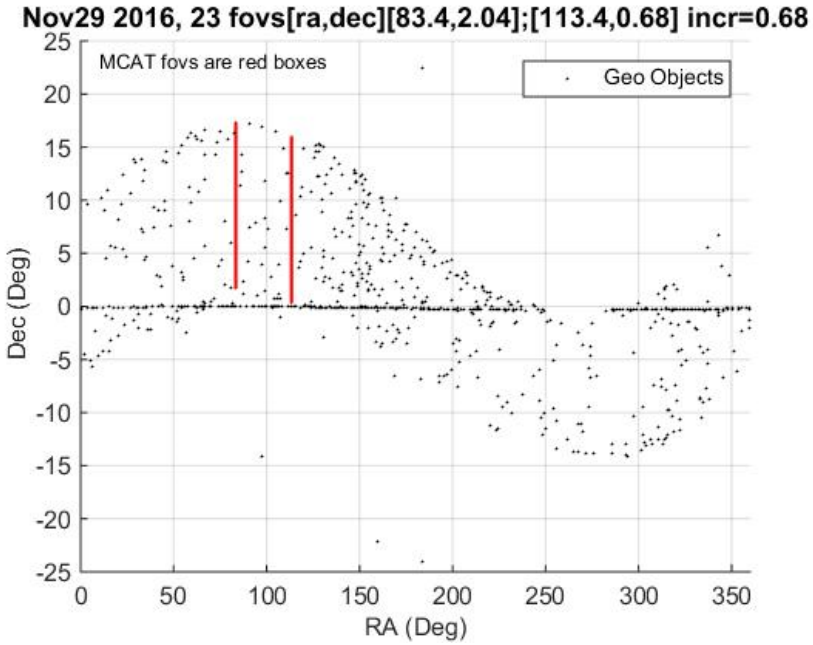

Fig. 3. The distribution of cataloged GEO objects for 29 November 2016. Twenty-three FOVs are stacked (appearing as two red bars) representing the pointings of the telescope at the first RA and the second RA, which is after the anti-solar point. Twenty-six FOVs were needed to cover the band at the first RA position due to that region being wider in declination space.

Using the above assumptions and methods, several simulations were performed to determine the orbital coverage different observing strategies could produce during a complete GEO belt survey. An initial one-month simulation covered only a part of the INC vs. RAAN space, so additional months were added to increase the coverage.

3.1 Quarterly Simulation

Observation campaigns described above were performed once every quarter during 2016 centered on the new moon dates of 8 March, 5 June, 1 September, and 29 November. A plot of the simulation results can be seen in Fig. 4. A color bar to the right of the main plot shows the EV value as it corresponds to a particular color. Significant gaps in the coverage, primarily above 20° in INC and at RAANs around 90°, 220°, and 310°, are easily seen as white regions. These regions represent the INC vs. RAAN locations that were not sampled using this observation strategy, which demonstrates this approach's shortcomings. The coverage between RAAN=90° and 270° is well below the desired value of EV =1.0.

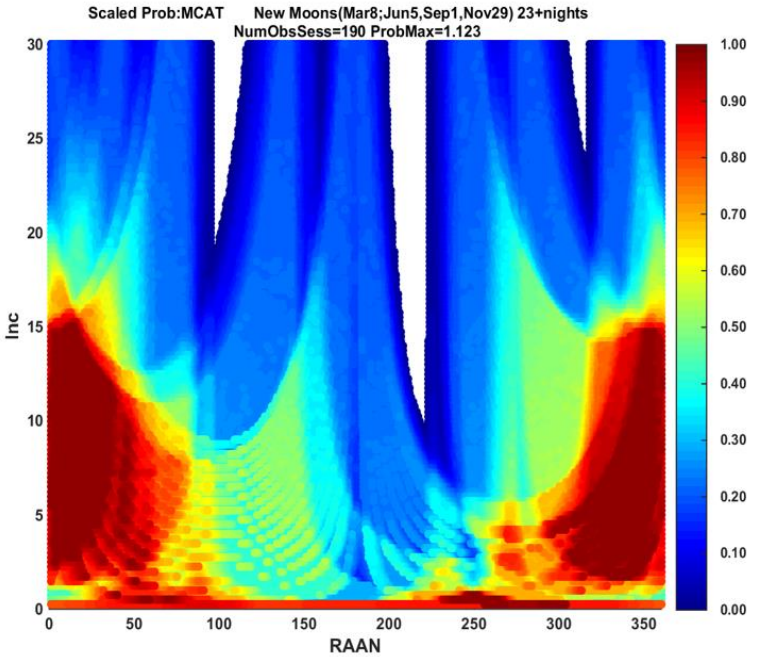

Fig. 4. Four months sampled on a quarterly basis. The white regions represented orbits that were not sampled using this method (EV=0). There are also many orbits of interest where the EV value is less than 1.0, implying this simulation was not sufficient.

3.2 Five Month Simulation

Another simulation was performed covering a 5-month period centered on the new moons in February, March, April, May, and June of 2016. These results can be seen in Fig. 4. This simulation resulted in a more complete spatial coverage (no white gaps, which represent orbital regimes that were not observed). However, there are many regions where the EV value is less than one. This can be seen near the 150° - 200° RAAN values.

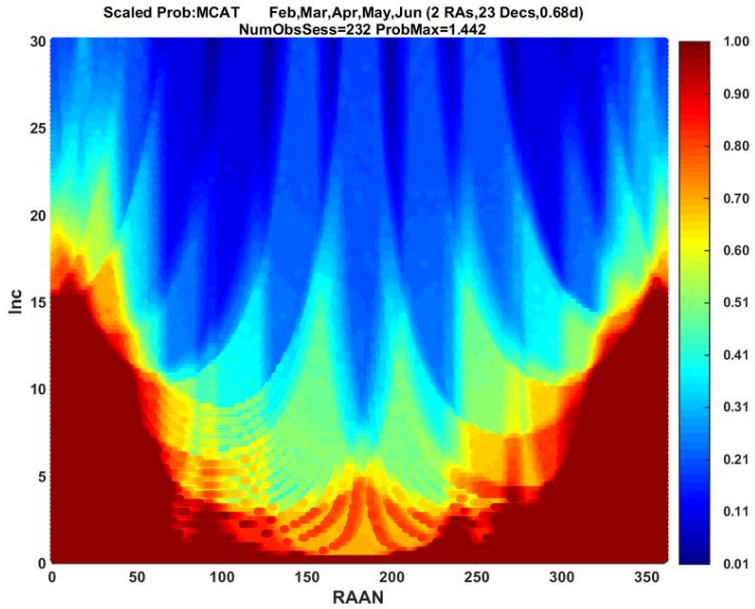

Fig. 5. GEO orbits sampled and EV values for observations during a 5 month, consecutive period. The unsampled white regions are no longer present, but there are still regions of interest that are under-sampled (have an EV < 1.0).

3.3 Six Month Simulation

Adding an additional month (6-month total) to the simulated observations shown in Fig. 5 produced a very similar plot. To check for seasonal effects, a simulation was carried out for a time period of 6 months, covering the new moons in July, August, 1 September, 30 September, October, and November. The resultant coverage can be seen in Fig. 6. Coverage is complete and very smooth and all densely populated regions of the GEO belt (see plotted data points in Fig. 2) are at or near an EV value of 1.0.

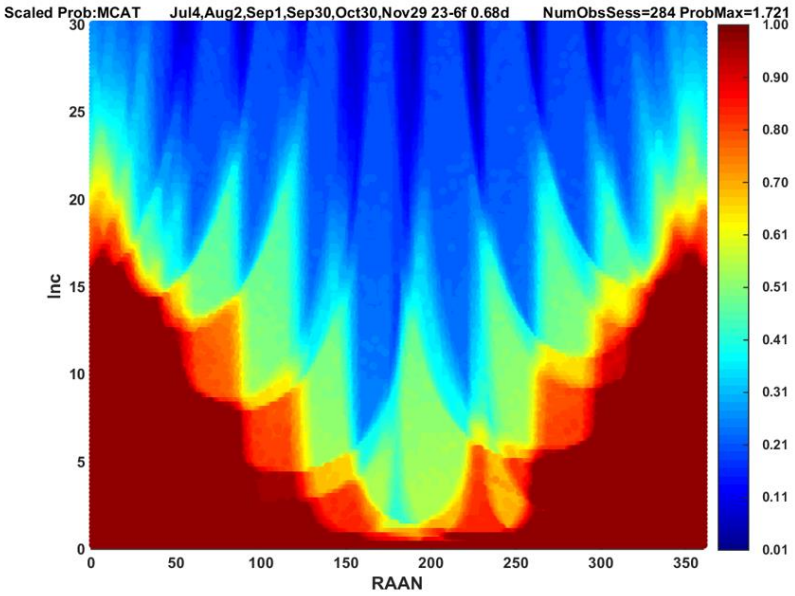

Fig. 6. The GEO coverage as shown in the previous figures but covering a consecutive, 6 month period beginning in July 2016. There are no un-sampled regions and the coverage is more smoothly sampled than in Fig. 5.

3.4 Future Simulations

Based solely on the simulations undertaken so far, a 5- to 6-month campaign will provide EV coverage $\geq$1.0 for nearly all regions of the INC vs. RAAN orbital space. However, these simulations have not considered important factors such as:

- Weather causing gaps in the 23 nights of continuous observational coverage;
- Effect of moonlight interference, which reduces the sensitivity of the camera system;
- Effects of observing within the galactic plane, which can add to the number of false detections; and
- Simulation assumptions that the anti-solar point was static from night to night instead of the actual slight movement in RA each night. This effect will broaden the coverage in RAAN.

These effects likely will increase the total time needed to produce a complete survey of the GEO region and will be the subject of future work.

4. Weather's Influence

In addition to future considerations mentioned in section 3.4, the simulations discussed throughout section 3 are not representative of actual observations since they do not account for observational time, data loss from cloud coverage, or unsafe observing conditions (rain, high winds, high humidity, *etc.*). The following section uses data collected by MCAT's weather sensors during 2016 as a guide to estimate future time loss due to inferior weather.

4.2 Weather Sensor Instrumentation

Weather data are collected at the MCAT facility on a 30-60 second cadence using a suite of eight instruments. These instruments include two Automated Systems Engineering (ASE) rain sensors, two Davis Vantage® PRO weather suites, two Boltwood Cloud Sensors (BCS), and two Optical Science Instruments (OSI) rain gauges. Rain is detected by the ASE rain sensors, the OSI rain gauges, and the BCS. Wind speed, relative humidity, and air temperature are measured by the Vantage PRO weather suites and the BCS. Cloud cover (based on the average sky temperature above the sensor) is also measured by the BCS. Since weather logs are generated by the automated system every night, results were compiled from data collected between March 2016 and July 2017 to determine how often the telescope could take scientifically relevant data if used on a nightly basis.

4.3 Weather Statistics

To determine if it is safe to open and operate the telescope (*i.e.*, certain weather criteria are met), the weather logs are analyzed every 30 seconds and determined whether the closure thresholds are reached. These dome closure thresholds include winds greater than 15.6 m/s (35 mph), relative humidity greater than 90%, and/or a detection of rain. The automation software maintains the dome closure for 20 minutes after a weather-related event. The combination of these time losses are added together and then divided by the total time the site is dark enough to observe (typically 12 hours on Ascension) to determine the percentage of lost time.

Another useful metric calculated from the weather instruments involves clouds detected with the BCS. If the BCS's sky temperature measurements suggest significant cloud cover is overhead, an additional close procedure is added. This is considered time the observatory would be closed or unable to take useful data. An additional ratio of down time is generated with this added condition and this metric is weighted based on how closely the two Boltwood sensors agree.

The possible operational uptimes averaged over each month are given below in Fig. 7. Included are results from the automated weather closing procedures (in orange) and the weighted average based on cloudiness measurements from the BCS. Notably, the southern summer solstice and autumnal equinox have the greatest amount of possible operational time while the least amount of clear uptime occurs during the southern winter solstice and spring equinox.

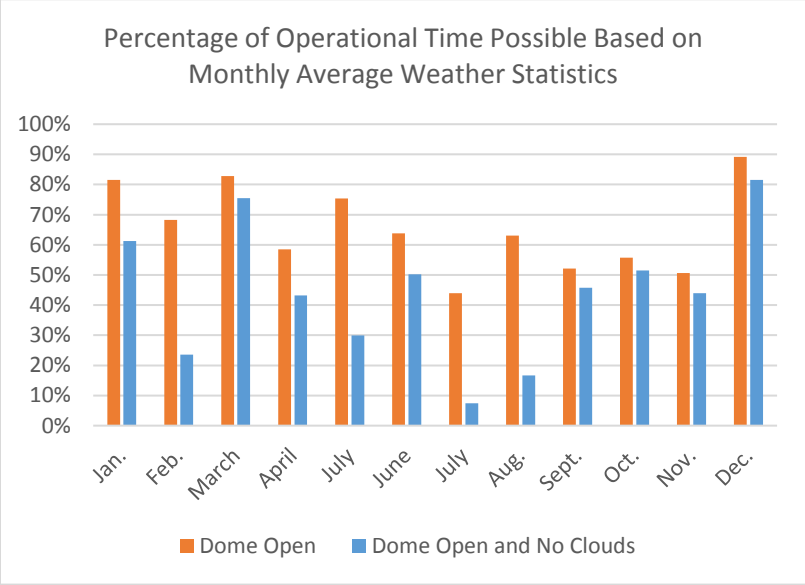

Fig. 7. Monthly average percentage times when the observatory would be open with (orange) and without (blue) clouds.

4.4 Implications

The simulations in Sec. 3 did not account for any estimation of cloud cover or dome closure due to weather. It was also determined that a time period of approximately 6 months is needed to complete a MODEST-like GEO survey with an EV value equal to or greater than one using MCAT's capabilities, assuming there are no nightly interruptions. If what is shown in this section is indeed typical weather to expect during a year on Ascension Island, and if the INC/RAAN coverage scales linearly with the amount of time available to observe, we estimate it will take roughly one year of observations to produce a GEO survey that is complete enough to use with the NASA models designed to calculate orbital debris population estimates (See [7]). It is useful to emphasize that these data represent what the authors would call "weather data" and not "climate data," given the relatively short time scale over which the data were collected. More weather data are being compiled and will be done so continuously during the life of MCAT to better estimate MCAT's typical uptime.

5. Towards Improving Initial Orbit Determination Accuracy

As in Section 1, due to the nature of the applied survey strategy, only a sparse number of angles-only data are collected and, as a result, a circular orbit has been assumed when performing the initial orbit determination for all of the detected objects. This assumption potentially causes a population of eccentrically orbiting objects moving at near-geosynchronous rates which would be incorrectly characterized.

To visualize this problem, a range of simulated objects were produced using Analytical Graphics' Systems Tool Kit (STK); each object having varying eccentricities, 0° inclination, the same apogee (42,000 km), and passing over MCAT during the same night. RAs and DECs for these objects were produced for every minute they were observable as well as their angular rates. These objects can be seen in Fig. 8 with their orbital element information listed in the table that follows.

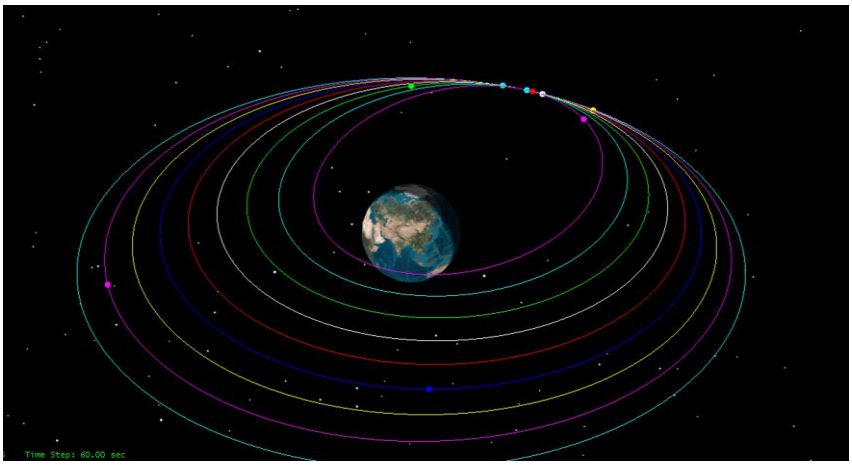

Fig. 8. Simulated resident space objects produced using STK. Each object has an apogee of 42,000 km with 0° inclination but varying perigee and eccentricities. A subset of these objects was used in initial Constrained Admissible Region, Multiple Hypothesis Filter (CAR-MHF) runs to demonstrate the need for a different survey strategy to characterize the objects with non-zero eccentricity.

Orbital Elements of the Simulated Objects used for the Preliminary CAR-MHF Runs

Obj	SMA	ECC	INC	ArgPer	RAAN	TrueAnom
Sat1	42000	0	0	0	0	0
Sat2	39900	0.053	0	0	0	0
Sat3	37800	0.111	0	0	0	0
Sat4	35700	0.176	0	0	0	0
Sat5	33600	0.25	0	0	0	0
Sat6	31500	0.333	0	0	0	0
Sat7	29400	0.429	0	0	0	0
Sat8	27300	0.538	0	0	0	0
Sat9	25200	0.667	0	0	0	0

Also discussed above, the observational strategy for MCAT involves obtaining a minimum of four detections of an object that is moving within a rate box specifically tuned for GEO rates (± 5 arcsec in RA and ± 2 arcsec in DEC) while surveying a particular region of space. These measurements come with some system-specific uncertainty associated with those measurements. Characterizing MCAT's uncertainties in these measurements is currently underway but they can be estimated from similar deployed systems. For these cases, assume a positional (RA/DEC) uncertainty measurement of +/- 1.5 arcsec.

Fig. 9 shows the angular rates in arcsec/sec of simulated space objects (Sat1, Sat3, and Sat9) with varying eccentricities that are observable over MCAT for the night of 1-2 February 2017. The solid lines are the angular rates of the objects themselves and the dashed lines with like colors are the estimated uncertainty bounds for calculating the angular rate based on the assumption of a 1.5 arcsec uncertainty in the measurement of an object's position. The red dashed lines represent the 'rate box' region such that objects within the bounds of those lines would be considered by the detection software to be potential GEO objects that are assigned a circular orbit estimation.

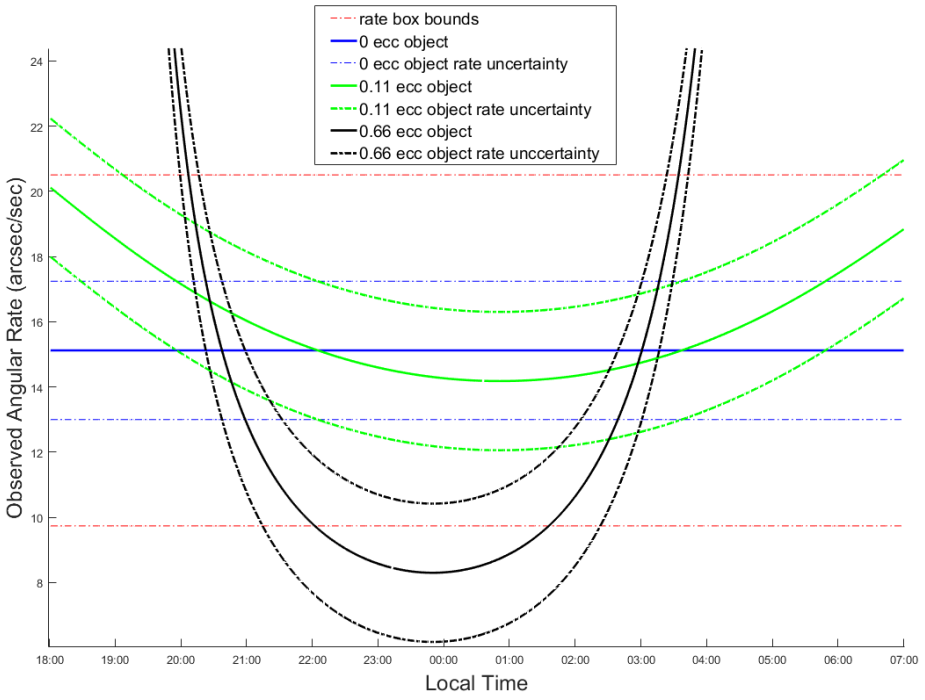

Fig. 9. The angular rate of simulated objects as they would appear over MCAT during one night of observing. Solid lines represent an object's angular rate and striped lines of the same color represent the estimated uncertainty for an angular rate measurement. The striped red lines represent the rate box bounds and define where an object needs to be in angular rate-space in order to be considered a GEO detection. Over the short time period in which a detection is made using the MODEST survey strategy discussed above, there is a large region of overlap where the detection of an object with an eccentric orbit could be classified as an object with low eccentricity, given the short observational window used in the current strategy (four observations in roughly 4 minutes).

Given adequate observations and sufficiently low uncertainties, observing a particular object's change in angular rate allows for convergence onto an initial orbit determination with reasonable uncertainties. However, the survey strategy described above would only obtain roughly four data points within a ~5-minute time frame. Fig. 9 shows multiple regions where the simulated objects would have similar observational characteristics over such a short period of time if only a circular orbit is fit to the observations.

Alternatively to assuming a circular orbit, the Constrained Admissible Region, Multiple Hypothesis Filter (CAR-MHF) as a more robust initial determination tool has been used with the simulated objects' observational data to attempt to recover their orbital information in a series of CAR-MHF runs.

CAR-MHF was developed specifically to perform initial orbit determination of targets using sparse, optical-angles only data such as those produced by MODEST and are expected to be produced by MCAT. It uses a joint probabilistic data association with backward smoothing and, as the name suggests, constrains the range of possible hypotheses to focus the filter into converging on a solution relevant to the user (the object is in orbit around the Earth, restricted to a range of semi-major axes, eccentricity, *etc.*). For specifics on the processes used with CAR-MHF, please see [8].

CAR-MHF runs have been done for the three objects in Fig. 9, restricting the observations to those consistent with the current survey strategy (5 min of RA/DEC observations per object per night). The preliminary results show that CAR-MHF cannot converge on a statistically significant solution with so few data points. This is because too many possible orbits that satisfy the constrained admissible region and the filter cannot prune enough of the hypotheses to produce a believable answer. Not surprisingly, this implies the need for an increase in the number of RA/DEC observations of the objects' orbital positions to generate an accurate initial determination.

To further this investigation, work is underway that manipulates the simulated observations of the above and other targets (changing inclination as well as eccentricity) before running the observations through CAR-MHF. This work varies the number of exposures per field, uncertainties in position, the number of revisits to the target (how many times the object needs are reacquired during the night) and other factors to provide insight into the limits and potential for conducting a survey that can determine eccentricities using MCAT and other telescopes.

6. PLANS FORWARD AND CONCLUSION

Simulations and collected weather data from Ascension Island have been presented to estimate the amount of time necessary for MCAT to produce an orbital debris survey of the GEO region. It was found that, in order to achieve sufficient INC/RAAN coverage, approximately 6 months of continuous nightly surveys are needed. The weather data that has been collected to date shows that roughly 50% of the observational time will either be lost due to bad weather or clouds, thus extending the 6-month estimate to roughly 1 year before a complete survey can be completed.

Additionally, the first steps toward developing a survey design that can efficiently and accurately obtain eccentricity information of the debris objects has been outlined. This analysis will be expanded to examine, in a more statistical sense, how MCAT can be used to sample more orbits that are eccentric. In a future paper, we will outline an updated observational strategy that, in addition to the traditional strategy, will account for more eccentric orbits using combinations of stare, detect, and chase methods, hand offs to other available sensors, and general observational cadence manipulation.

7. ACKNOWLEDGEMENTS

The authors would like to acknowledge the help of the CAR-MHF team at the Air Force Research Lab's Space Vehicles Directorate for their help in obtaining and using the CAR-MHF software.

8. REFERENCES

1. Friesen, L. *et al*., "Results in Orbital Evolution of Objects in the Geosynchronous Region," AIAA 90-1362, AIAA/NASA/DOD Orbital Debris Conference: Technical Issues and Future Directions, Baltimore, MD, 1990.
2. Vaughan, S. H. and Mullikin, T. L., "Long Term Behavior of Inactive Satellites and Debris Near Geosynchronous Orbits," AIAA 95-200, AAS/AIAA Spaceflight Mechanics Meeting, Albuquerque, NM, 1995.
3. Abercromby, K., Seitzer, P., Barker, E., Rodriguez, H., and Matney, M., "A Summary of Five Years of Michigan Orbital Debris Survey Telescope (MODEST) Data," 2008 IAC, Glasgow, Scotland, 29 September-3 October 2008.
4. Abercromby, K., Seitzer, P., Cowardin, H., Barker, E., Matney, M., Michigan Orbital DEbris Survey Telescope Observations of the Geosynchronous Orbital Debris Environment Observing Years: 2007-2009, Final Report, NASA/TP-2011-217350, September 2011.

5. Matney, M., Barker, E., Seitzer, P., Abercromby, K., and Rodriguez, H., Calculating Statistical Orbit Distributions using GEO Optical Observations with the Michigan Orbital Debris Survey Telescope (MODEST), 57th International Astronautical Congress, Valencia, Spain, 2-6 Oct. 2006.
6. Mulrooney, M., Hickson, P., and Stansbery, E., Orbital Debris Detection and Tracking Strategies for the NASA/AFRL Meter Class Autonomous Telescope (MCAT)," 61st International Astronautical Congress, Prague, Czech Republic, 27 Sep. – 1 Oct. 2010.
7. S. M. Lederer, P. Hickson, H. M. Cowardin, B. Buckalew, J. Frith, R. Alliss, NASA's Optical Program on Ascension Island: Bringing MCAT to Life as the Eugene Stansbery-Meter Class Autonomous Telescope (ES-MCAT), AMOS Technical Conference 2017 (to be submitted Sep 2017)
8. Stauch, J., Jah, M., Baldwin, J., Kelecy, T., Hill, K.A., "Mutual Application of Joint Probabilistic Data Association, Filtering, and Smoothing Techniques for Robust Multiple Space Object Tracking", AIAA/AAS Astrodynamics Specialist Conference 2014, 10.2514/6.2014-4365., 2014.